Multiplexing of optical fiber gas sensors with a frequency-modulated continuous-wave technique

H. B. Yu, W. Jin, H. L. Ho, K. C. Chan, C. C. Chan, M. S. Demokan, G. Stewart, B. Culshaw, and Y. B. Liao

We report on the use of a frequency-modulated continuous-wave technique for multiplexing optical fiber gas sensors. The sensor network is of a ladder topology and is interrogated by a tunable laser. The system performance in terms of detection sensitivity and cross talk between sensors was investigated and found to be limited by coherent mixing between signals from different channels. The system performance can be improved significantly by use of appropriate wavelength modulation–scanning coupled with low-pass filtering. Computer simulation shows that an array of 37 acetylene sensors with a detection accuracy of 2000 parts in 10^6 for each sensor may be realized. A two-sensor acetylene detection system was experimentally demonstrated that had a detection sensitivity of 165 parts in 10^6 for 2.5-cm gas cells (or a minimum detectable absorbance of 2.1×10^{-4}) and a cross talk of -25 dB. © 2001 Optical Society of America

OCIS codes: 060.2370, 060.4230, 060.2630, 300.1030, 300.6340, 300.6380.

1. Introduction

As a result of the development of advanced laser sources and signal measurement techniques, weak gas absorption in the near-IR band can be detected by fiber-coupled micro-optic cells with high sensitivity.[1] A number of important gases, including methane, acetylene, hydrogen sulfide, and carbon dioxide, that possess overtone or combination absorption lines in the transmission windows of silica fibers can be detected with the same type of fiber gas sensor system.[2–9] Compared with conventional gas detection systems, fiber optic systems offer a number of advantages, including immunity to electromagnetic fields, intrinsic safety in hazardous environments, remote detection, and distributed network capabilities.

Tunable laser sources including distributed-feedback lasers and tunable external-cavity semiconductor lasers are important sources of fiber optic gas sensors. The special features of these lasers include the ability to modulate and tune the laser wavelength and the high spectral power densities within a linewidth that is narrower than a single gas absorption line.[8–12] The laser sources can enhance the selectivity and sensitivity of optical gas sensors more than LED's can. The high spectral power density of the lasers would also permit, while keeping the reasonable sensitivity that applications allow, multiplexing of a network of gas sensors that share the same source and other expensive optoelectronic components. This would reduce the cost per sensing point and enhance the competitiveness compared with conventional electrical–chemical gas sensors. Spatial division multiplexing[13] (SDM) and time-division multiplexing[14] (TDM) techniques have been used for multiplexing fiber optic gas sensors. The SDM system exhibits a performance similar to that of a single-cell system, but a number of receivers and signal processing units need to be used. The TDM system uses a single source-and-receiver unit and thus potentially has a lower cost. But the pulsing of light from the laser source in the TDM system does not make good use of laser power and would result in a poor signal-to-noise ratio if a number of sensors were multiplexed. Furthermore, the limited extinction ratio of the optical switch used in the TDM system would result in cross talk and affect the system's perfor-

H. B. Yu and Y. B. Liao are with the Department of Electronic Engineering, Tsinghua University, Beijing 100084, China. H. B. Yu is also with and W. Jin H. L. Ho (eehlho@ee.polyu.edu.hk), K. C. Chan, C. C. Chan, and M. S. Demokan are with the Department of Electrical Engineering, The Hong Kong Polytechnic University, Kowloon, Hong Kong, China. G. Stewart and B. Culshaw are with the Department of Electronic and Electrical Engineering, University of Strathclyde, Glasgow G1 1XW, UK.

Received 19 May 2000; revised manuscript received 24 August 2000.
0003-6935/01/01011-10$15.00/0

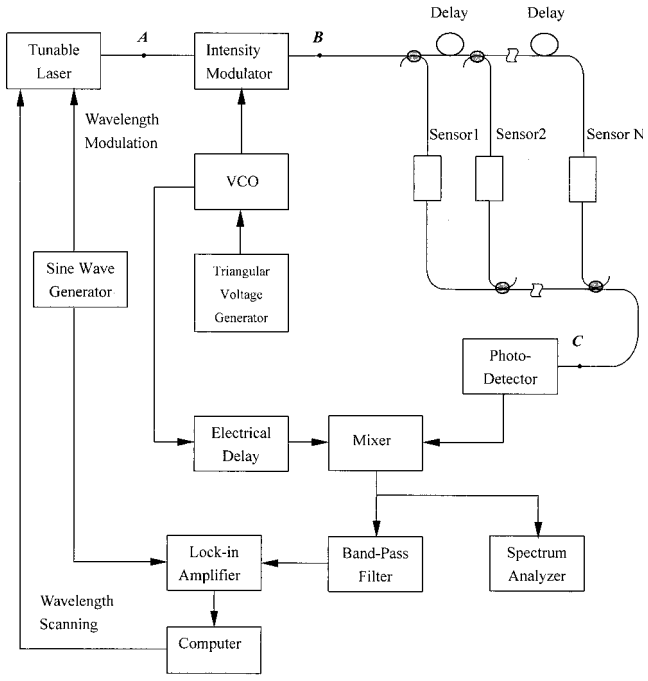

Fig. 1. FMCW multiplexed ladder gas-sensor array.

mance. High-extinction-ratio optical switches are required for good system performance.[14–16].

Frequency-modulated continuous-wave (FMCW) modulation[17,18] has a higher duty cycle than TDM and thus would provide a better signal-to-noise ratio at the system output. However, the technique has not been fully examined, to the authors' knowledge, for efficiency in multiplexing fiber gas sensors. In this paper we report on the results of our recent investigations in applying the FMCW technique for addressing fiber gas sensors. The theory of using a FMCW for multiplexing a number of gas sensors connected in a ladder topology is presented in Section 2. The use of wavelength-modulation spectroscopy for the FMCW multiplexed sensor array and the modulation characteristics of the unwanted interferometric signals are investigated in Section 3. Methods for minimizing the effects of interferometric signals are presented in Section 4. The effect of nonzero sidelines of the FMCW technique on the system performance is investigated in Section 5. The results of experimental investigations are given in Section 6, and a summary in Section 7.

2. Theory of the Frequency-Modulated Continuous Wave for Multiplexing Fiber Optic Gas Sensors

Figure 1 shows the FMCW multiplexed gas sensor array. The system consists of N transmission-type gas cells connected in a forward-coupled ladder topology.[14] Light from the tunable laser source is modulated in intensity through the use of an external intensity modulator with a triangular chirped frequency carrier generated from a voltage-controlled oscillator and coupled into the gas sensor array. When light passes through the gas cells, gas concentration information is encoded onto the light intensity. The return light signals from different sensors are coupled into a common output fiber and then converted into electric signals by a high-speed photodetector and subsequently mixed with a reference signal from the voltage-controlled oscillator (VCO). The output from the mixer will consist of N beat notes (corresponding to N sensors), with their respective beat frequencies determined by the time-delay differences between the sensor and the reference signals.

The spectrum of a beat note signal usually consists of a set of discrete spectral lines. Under the ideal conditions that (1) the signals from different channels are incoherent and (2) the time delay difference (τ_i, $i = 1, 2, \ldots, N$) between the sensor and the reference channels and the parameters of the triangular chirped carrier, i.e., the angular frequency excursion $\Delta\omega$ and the average angular frequency of ω_0, satisfy

$$\Delta\omega\tau_i = k\pi, \tag{1}$$

$$\omega_0\tau_i = \frac{k\pi}{2} + l\pi, \tag{2}$$

where k and l are integers, the spectrum of the ith beat note will be approximately a single line at $\omega_i = k\omega_s$. Here, $\omega_s = 1/T_s$; T_s is the period of the triangular chirping. The amplitude of the spectral line at $k\omega_s$ will be (see Appendix A)

$$V_i(\omega_i = k\omega_s) \approx \chi I_A \exp[-2\alpha(\nu)C_iL], \tag{3}$$

where χ is a constant that depends on a number of parameters as described in the Appendix A. I_A is the light intensity from the laser at point A, as indicated in Fig. 1. $\alpha(\nu)$ is the amplitude absorption coefficient of the gas. ν represents the laser frequency and is related to wavelength by $\nu = c/\lambda$. C_i is the gas concentration at the ith sensor. L is the length of the gas cells. For simplicity, we have assumed that all the gas cells are of the same length.

If we can design the delay difference τ_i such that each sensor corresponds to a different value of k, we may be able to multiplex a number of sensors in the frequency domain. The sensor signals may be separated (demultiplexed) by use of electronic bandpass filters of appropriate passing bands.

In practice, there would be unwanted interferometric signals owing to coherent mixing of light waves from different channels that would result in an additional term in the output of sensor i (at $\omega_i = k\omega_s$). The amplitude of this term is (Appendix A)

$$V_{i,n}(\omega_i = k\omega_s) = \chi I_A \sum_{j=1, j\neq 1}^{N} \exp[-\alpha(\nu)(C_i + C_j)L] \times (\cos \Delta\psi_{ij})_B, \tag{4}$$

where $\Delta\psi_{ij}$ represents a phase difference between the light signals from channels i and j. $(\cos \Delta\psi_{ij})_B$ represents the low-frequency component of $\cos \Delta\psi_{ij}$ that passes the bandpass filter center at $k\omega_s$. To see the effect of this unwanted interferometric term on the system performance, we consider a simple case in

which no wavelength modulation or tuning is applied. The phase difference $\Delta\psi_{ij}$ can now be expressed as $\Delta\psi_{ij} = 2\pi\nu_{L0}(\tau_j - \tau_i) + \Delta\phi_{ij}$, where ν_{L0} is the laser frequency. This phase difference varies randomly at relatively low frequency as a result of environmental disturbance $\Delta\phi_{ij}$ and causes $(\cos \Delta\psi_{ij})_B$ to vary from 1 to -1 if the change in $\Delta\psi_{ij}$ is beyond 2π. The signal given in Eq. (4) would then vary significantly compared with the sensor signal as given in expression (3), making detection of small gas concentrations difficult, if not impossible.

Apart from its sensitivity to the unwanted interferometric signals, the performance of the gas sensor array is also affected by various kinds of noise such as source and shot noise and the effect of a time-varying polarization state. All these were analyzed in a previous paper for a TDM system.[13] For the FMCW system reported here, the effect of polarization variation and the source noise will be more-or-less the same as that for the TDM system. The shot-noise-limited performance should be better than that of the TDM system because of the relatively high average power level associated with the FMCW system. The effect of the shot and the source noise is, however, much smaller than that of the unwanted interferometric signals.[13]

3. Wavelength-Modulation Spectroscopy in the Frequency-Modulated Continuous-Wave System

Gas concentration C_i can be recovered from expression (3) by further processing of signal $V_i(\omega_i = k\omega_s)$ after demultiplexing. The processing method includes direct measurement of the signal magnitude from the bandpass filter while the laser wavelength is locked to a gas absorption line by use of a reference gas cell[9,12] and measurement of the variation in the signal amplitude when the laser wavelength is scanned across a gas absorption line.[7] In this section we examine the use of a wavelength-modulation spectroscopy technique in which the laser wavelength is modulated sinusoidally at a relatively higher frequency while the average wavelength is locked to or scanned across a gas absorption line. The second harmonic of the wavelength modulation is detected with a lock-in amplifier and used as a measure of gas concentration.[7–10]

Assume that the laser frequency (wavelength) is sinusoidally modulated; i.e., that

$$\nu(t) = \nu_{L0} + \nu_{Lm} \sin \omega_m t, \tag{5}$$

where ν_{L0} and ν_{Lm} are, respectively, the laser average frequency and the amplitude of wavelength modulation, $\omega_m = 2\pi f_m$, and f_m is the frequency of the wavelength modulation. As the laser wavelength modulation is usually accompanied by residual intensity modulation, the light intensity from the laser (at point A as indicated in Fig. 1) will be time varying and may be written as

$$I_A(t) = I_0(1 + \eta \sin \omega_m t), \tag{6}$$

where η is the residual intensity modulation index and I_0 is the average light intensity from the source. Substituting Eqs. (5) and (6) into expression (3), we obtain

$$V_i(\omega_i = k\omega_s) = \chi I_0[1 + \eta \sin(\omega_m t)] \times \exp[-2\alpha(\nu_{L0} + \nu_{Lm} \sin \omega_m t)C_i L]. \tag{7}$$

The gas absorption line under atmospheric pressure is collision broadened and is given by[9]

$$\alpha(\nu) = \frac{\alpha_0}{1 + [(\nu - \nu_g)/\delta\nu)]^2}, \tag{8}$$

where α_0 represents the amplitude absorption coefficient for pure gas at the center of the absorption line and ν_g and $\delta\nu$ are, respectively, the center frequency and the half-width of the absorption line. The second harmonic of the modulation signal can be obtained by expansion of Eq. (7) into a Fourier series of ω_m. The second harmonic is maximized when the average wavelength of laser is at the center of the gas line ($\nu_{L0} = \nu_g$) and may be expressed as[9]

$$V_{i,2\omega_m} \approx -2\chi I_0 k_0 \alpha_0 C_i L, \tag{9}$$

with

$$k_0 = \frac{(1 - \sqrt{1 + x^2})^2}{x^2\sqrt{1 + x^2}}, \tag{10}$$

where x is defined as

$$x = \nu_{Lm}/\delta\nu. \tag{11}$$

Expression (9) is the output that corresponds to sensor i and is similar to the formula for the single gas sensor system.[9]

The second harmonic of the unwanted interferometric signal for sensor i can be obtained by substitution of Eqs. (5) and (6) into Eq. (4) and is expressed as (Appendix A)

$$V_{i,n,2\omega_m}(\omega_i = k\omega_s) = \chi I_0 \sum_{j=1, j\neq i}^{N} [(\cos \xi_{ij} \times M_{s,ij} + \eta \sin \xi_{ij} \times M_{0,ij}) + \cos \xi_{ij} \times \alpha_0 C_i L \times M_{c,ij} + \cos \xi_{ij} \times \alpha_0 C_j L \times M_{c,ij}], \tag{12}$$

with

$$M_{c,ij} = \frac{-x^2 J_2(\zeta_{ij})}{(1 - \sqrt{1 + x^2})^2} - [J_0(\zeta_{ij}) + J_4(\zeta_{ij})] - [J_2(\zeta_{ij}) + J_6(\zeta_{ij})]\left[\frac{2}{x^2} - \frac{1}{2(1 - \sqrt{1 + x^2})^2}\right], \tag{13}$$

$$M_{0,ij} = -[J_1(\zeta_{ij}) - J_3(\zeta_{ij})]\frac{x^2\sqrt{1 + x^2}}{(1 - \sqrt{1 + x^2})^2}, \tag{14}$$

$$M_{s,ij} = -J_2(\zeta_{ij})\frac{x^2\sqrt{1 + x^2}}{(1 - \sqrt{1 + x^2})^2}, \tag{15}$$

$$\xi_{ij} = 2\pi \int_{t-\tau_{ji}}^{t} \nu_{L0}(t)\mathrm{d}t + \Delta\phi_{ij}, \tag{16}$$

$$\zeta_{ij} = \frac{4\pi\nu_{Lm}}{\omega_m} \sin(\omega_m\tau_{ji}/2) \approx 2\pi\nu_{Lm}\tau_{ji}, \tag{17}$$

where $\tau_{ji} = \tau_j - \tau_i$ represents a delay time difference between the signals from sensors j and i.

4. Minimization of the Unwanted Interferometric Signals

A. Wavelength-Modulation Technique

Equation (12) gives the second harmonics $V_{i,n,2\omega_m}$ ($\omega_i = k\omega_s$) of the unwanted interferometric signals. We now look at how these signals affect the sensor performance in terms of minimum detectable gas concentration. $V_{i,n,2\omega_m}$ ($\omega_i = k\omega_s$) includes three terms. The second term is proportional to C_i, vanishes when C_i tends to zero, and therefore will not set a limit on the detection sensitivity of sensor i. The first term is independent of gas concentration and will set a limit to the detection sensitivity. By setting this term to be equal to the signal given in expression (9) we obtain the detection sensitivity of sensor i in terms of minimum detectable gas concentration as

$$C_{i,\min 1} = \frac{\sum_{j=1,j\neq i}^{N} (M_{s,ij}\cos\xi_{ij} + M_{0,ij}\eta\sin\xi_{ij})}{2\alpha_0 L k_0} \approx \frac{\sum_{j=1,j\neq i}^{N} M_{s,ij}\cos\xi_{ij}}{2\alpha_0 L k_0}, \tag{18}$$

where we have neglected the $M_{0,ij}\eta\sin\xi_{ij}$ term because it very small (η is very small). The root-mean-square (rms) value of $C_{i,\min 1}$ is

$$[C_{i,\min 1}]_{\mathrm{rms}} \approx \frac{\left[2\sum_{j=1,j\neq i}^{N} (M_{s,ij})^2\right]^{1/2}}{4\alpha_0 L k_0} \leq \frac{\sqrt{2(N-1)}\, M_{s,\max}}{4\alpha_0 L k_0}, \tag{19}$$

where the rms value of $\cos\xi_{ij}$ has been taken as $1/\sqrt{2}$. $M_{s,\max}$ represents the maximum value of $M_{s,ij}$. The third term is proportional to C_j and will cause cross talk to sensor i. By setting this term to be equal to the right-hand side term in expression (9), we obtain the cross-talk performance of sensor i as

$$C_{i,\min 2} \approx \frac{\sum_{i=1,j\neq i}^{N} C_j M_{c,ij}\cos\xi_{ij}}{2k_0}; \tag{20}$$

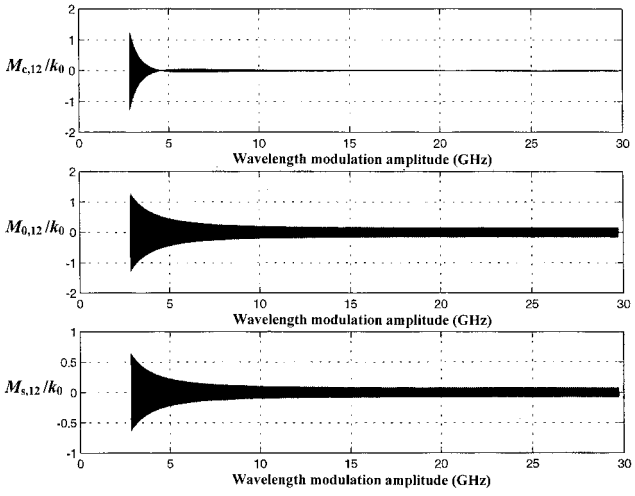

Fig. 2. $M_{s,12}/k_0$, $M_{0,12}/k_0$, and $M_{c,12}/k_0$ as functions of ν_{Lm}.

the corresponding rms value is

$$[C_{i,\min 2}]_{\mathrm{rms}} \approx \frac{\left[2\sum_{i=1,i\neq j}^{N} C_j^2 M_{c,ij}^2\right]^{1/2}}{4k_0} \leq \frac{\sqrt{2(N-1)}\, M_{c,\max} C_{\max}}{4k_0}, \tag{21}$$

where $C_{\max}$ is the upper limit of the gas concentration and $M_{c,\max}$ represent the maximum values of $M_{c,ij}$.

As ζ_{ij} is a function of ν_{Lm}, $M_{c,ij}$, $M_{0,ij}$, and $M_{s,ij}$ are also functions of ν_{Lm}. We take the case for $i = 1$ and $j = 2$ as an example. $M_{c,12}/k_0$, $M_{0,12}/k_0$, and $M_{s,12}/k_0$ as functions of ν_{Lm} were calculated from Eqs. (13)–(15) and Eq. (11) and are shown in Fig. 2. During the calculation we assumed that $f_m = 500$ Hz and $\tau_{21} = 100$ ns. As shown in Fig. 2, all three parameters are rapidly oscillating when ζ_{ij} or ν_{Lm} is varied. Any small variation in wavelength or path length would therefore significantly affect the values of these parameters. It is therefore meaningful to look only at the envelope of these oscillations. The (envelope) values of $M_{0,12}/k_0$ and $M_{s,12}/k_0$ are of the same order and decrease with an increase of ν_{Lm}. $M_{c,12}/k_0$ follows a similar trend but decreases much faster and to a much smaller value than do $M_{0,12}/k_0$ and $M_{s,12}/k_0$. Near $\nu_{Lm} = 22$ GHz, the maximum value of $M_{c,12}/k_0$ is $\sim 4 \times 10^{-3}$; the values of $M_{0,12}/k_0$ and $M_{s,12}/k_0$ are ~ 0.08.

Expressions (19) and (21) can be used to estimate the performance of a gas measurement system in which the average wavelength of the laser is locked at the center of the gas absorption line [i.e., $\nu_{L0}(t) \equiv \nu_g$]. The value of ξ_{ij} under this condition may be written as

$$\xi_{ij} = 2\pi \int_{t-\tau_{ji}}^{t} \nu_{L0}(t)\mathrm{d}t + \Delta\phi_{ij} = 2\pi\nu_{L0}\tau_{ji} + \Delta\phi_{ij}. \tag{22}$$

ξ_{ij} varies randomly within a low-frequency range as a result of environmentally induced phase change $\Delta\phi_{ij}$. For gas sensors with wavelengths tuned across the gas absorption, the measurement accuracy may be further enhanced by use of an appropriate low-pass filter, as we discuss in Subsection 4.B.

B. Low-Pass Filtering Technique

It can be seen from expressions (18) and (20) that the measurement errors are proportional to cos ξ_{ij}. If the laser wavelength (frequency ν_{L0}) is scanned linearly across the gas absorption line, cos ξ_{ij} will vary periodically with time. If the time delay τ_{ji} is sufficiently large that variation of ξ_{ij} ($=2\pi\nu_{L0}\tau_{ji} + \Delta\phi_{ij}$) is many times π, cos ξ_{ij} will vary much faster than the absorption signal and can therefore be removed by use of a low-pass filter. This indicates that one could achieve much higher sensitivity by combining wavelength scanning with the use of a low-pass filter. This technique has actually been applied in gas absorption spectroscopy to minimize unwanted etalon effects.[19]

When the laser is scanned, the laser average frequency $\nu_{L0}(t)$ may be expressed as

$$\nu_{L0}(t) = \nu_{La} + B_{Lb}t, \qquad t \in (0, T), \tag{23}$$

where T is the period of wavelength scanning and is typically of the order of one or tens of seconds. ν_{La} is the lowest average frequency, and B_{Lb} is the slope of the wavelength scanning.

Equation (16) may be rewritten as

$$\xi_{ij} = 2\pi \int_{t-\tau_{ji}}^{t} \nu_{L0}(t)\mathrm{d}t + \Delta\phi_{ij} = 2\pi B_{Lb}\tau_{ji}t + 2\pi(\nu_{La} - \tfrac{1}{2}B_{Lb}\tau_{ji})\tau_{ji} + \Delta\phi_{ij}, \tag{24}$$

$$\cos\xi_{ij} = \cos(2\pi B_{Lb}\tau_{ji}t + \phi_0 + \Delta\phi_{ij}), \tag{25}$$

where $\phi_0 = 2\pi(\nu_{La} - \tfrac{1}{2}B_{Lb}\tau_{ji})\tau_{ji}$ is a constant.

Assume that a lock-in amplifier is used to detect the second-harmonic signal. As the lock-in amplifier may be regarded as a narrow-bandpass filter, only signals with frequencies near $2f_m$ (±several hertz) can pass through. Therefore only the dc component of cos ξ_{ij} can appear at the output of the lock-in amplifier, and expressions (18) and (20) can then be rewritten as

$$C_{i,\min 1} \approx \frac{\sum_{j=1,j\neq i}^{N} M_{s,ij}(\cos\xi_{ij})_{\mathrm{dc}}}{2\alpha_0 L k_0} \leq \frac{(N-1)M_{s,\max}(\cos\xi_{ij})_{\mathrm{dc,max}}}{2\alpha_0 L k_0}, \tag{26}$$

$$C_{i,\min 2} \approx \frac{\sum_{j=1,j\neq i}^{N} C_j M_{c,ij}(\cos\xi_{ij})_{\mathrm{dc}}}{2k_0} \leq \frac{(N-1)C_{\max}M_{c,\max}(\cos\xi_{ij})_{\mathrm{dc,max}}}{2k_0}, \tag{27}$$

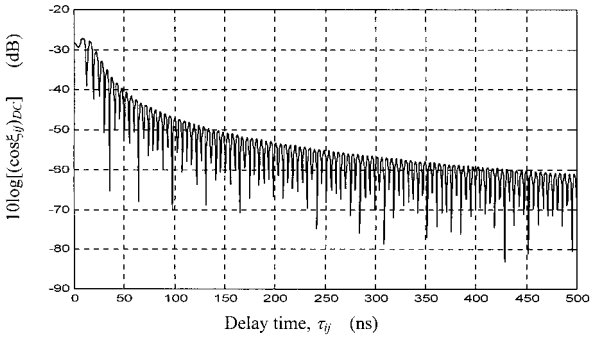

Fig. 3. dc component of cos ξ_{ij} as a function of time-delay difference τ_{ji} between sensors.

where $(\cos\xi_{ij})_{\mathrm{dc}}$ represents the dc component of cos ξ_{ij}. A computer simulation was made to calculate the value of $(\cos\xi_{ij})_{\mathrm{dc}}$ as a function of delay time τ_{ij} for an arbitrary set of parameters: ν_{La} = 19 608 GHz (1530 nm), B_{Lb} = 2.7 GHz/s, T = 15 s, $\phi_0 = 0$, and $\Delta\phi = 0$. The values of $(\cos\xi_{ij})_{\mathrm{dc}}$ as a function of time-delay difference τ_{ij} between sensors are shown in Fig. 3. The vertical axis $10\log|(\cos\xi_{ij})_{\mathrm{dc}}|$ expresses the value of the dc component of cos ξ_{ij} in units of decibels. For a 20-m delay between sensors, corresponding to $\tau_{ji} \approx 100$ ns, the maximum value of $(\cos\xi_{ij})_{\mathrm{dc}}$ is found to be 47 dB smaller than that of the value of cos $\xi_{ij} = 1$, indicating that the detection sensitivity can be improved by 47 dB by wavelength scanning and lock-in detection. However, as we are now dealing with a fiber optic system, environmental variation may affect the fiber length and the index and therefore result in random variation of the phase $\Delta\phi_{ij}$. This phase variation would affect the efficiency of noise reduction[20] with lock-in detection and would limit the improvement factor to ~30 dB instead of the 47 dB as mentioned above.

The maximum possible value of $C_{i,\min 1}$ as a function of sensor number was calculated from expression (26) and is shown as curve a of Fig. 4. During the calculation, the values of $10\log|(\cos\xi_{ij})_{\mathrm{dc,max}}|$, α_0, and L were taken as −30 dB, 0.5 cm^{-1}, and 2.5 cm, re-

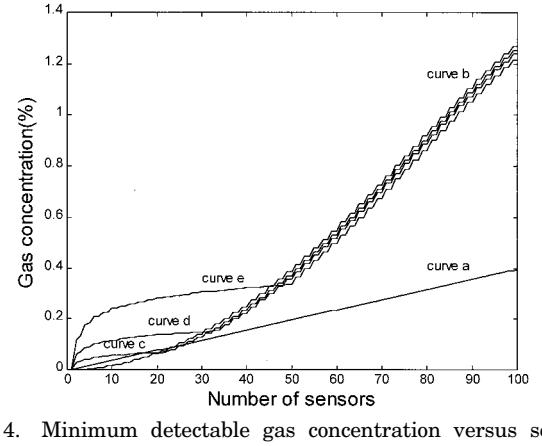

Fig. 4. Minimum detectable gas concentration versus sensor number: curve a, the interferometric effect; curves b–e, the effect of the sideline of FMCW.

spectively. The cross-talk effect $C_{i,\min 2}$ calculated from expression (27) was found to be much smaller than $C_{i,\min 1}$ and is not shown. It should be mentioned that curve a is an estimate of the upper limit of $C_{i,\min 1}$ based a simplified formula [expression (26)]. The actual value of $C_{i,\min 1}$ could be smaller than that given in curve a. The detection sensitivity in terms of minimum detectable gas concentration $C_{i,\min 1}$ as limited by the unwanted interferometric signals [expression (26) and curve a of Fig. 4] is inversely proportional to α_0 and L. One can also express it in terms of minimum detectable absorbance by simply multiplying $C_{i,\min 1}$ by $\alpha_0 L = 0.5 \times 2.5 = 1.25$. For example, as many sensors as 50, $C_{i,\min 1}$ as shown in Fig. 4 (curve a) is less than 0.2% [2000 parts in 10^6 (ppm)], corresponding to a minimum detectable absorbance of 2000 ppm $\times$ 1.25 = 2.5×10^{-3}.

5. Cross-Talk Performance Resulting from the Sidelines of the Frequency-Modulated Continuous-Wave System

As discussed in Section 2, a signal from each sensor would consist of a set of discrete lines in the frequency domain with frequency interval ω_s. If the modulation and the system parameters are selected carefully according to Eqs. (1) and (2), the signal from any particular sensor will have an approximately single line spectrum. For a single sensor system, this can easily be achieved by adjustment of ω_0, $\Delta\omega$, and τ. For a multiple-sensor system, ω_0 and $\Delta\omega$ are usually fixed, and Eqs. (1) and (2) may not be satisfied accurately because of the error in controlling the length of the fiber delay lines. Any mismatch or bias from Eqs. (1) and (2) would increase the magnitude of the sidelines, which implies that the signal at a particular frequency would include not only the beat signal from the sensor of interest but also the sidelines from other neighboring sensors. These nonzero sidelines would cause cross talk between sensors and affect measurement accuracy.[17,18]

The detection accuracy of sensor i as limited by the FMCW sideline is (Appendix A):

$$[C_{i,\text{cross}}^{N}]_{\min} = \frac{2\sum_{j=1,j\neq i}^{N} M_j C_j}{T_s} \approx \frac{2}{T_s}\sum_{j=1,j\neq i}^{N} M_j C_j \leq \frac{2}{T_s} \times \max\left(\sum_{j=1,j\neq i}^{N} M_j C_j\right), \tag{28}$$

with M_j is defined as

$$M_j = -\frac{\sin[(\Delta\omega/T_s)(\tau_i - \tau_j)(\tfrac{1}{2}T_s - \tau_j)]}{(\Delta\omega/T_s)(\tau_i - \tau_j)} \cos(\omega_0\tau_j - \tfrac{1}{2}\Delta\omega\tau_i), \tag{29}$$

where C_j is in the range from 0–$C_{\max}$. The sensor performance in terms of minimum detectable gas concentration owing to cross talk from the nonzero sidelines as functions of sensor numbers is evaluated with Eq. (28) and is shown in Fig. 4 as curves b–e. The maximum gas concentrations for all the sensors are assumed to be the same and equal to $C_{\max} = 5\%$. Curve b is obtained under the ideal condition when Eqs. (1) and (2) are satisfied. Curves c, d, and e are for cases when the time-delay bias from Eqs. (1) and (2) equal 0.025, 0.05, and 0.1 ns, respectively, corresponding to fiber lengths of 0.5, 1, and 2 cm, respectively.

In summary, the interferometric effect is dominant and will set a limit on the system performance when Eqs. (1) and (2) are satisfied and the number of sensors is fewer than 23. However, for a small number of sensors (as many as 17 for 0.5-cm bias; Fig. 4, curve c), if Eqs. (1) and Eq. (2) are not satisfied, the sideline effect associated with the FMCW technique may exceed the interferometric effect. From Fig. 4 we can see that it should be possible to achieve 2000 ppm (0.2%) accuracy for as many as 37 sensors when the bias of the delay fiber length is less than 1 cm (curve d).

It should be mentioned that the detection accuracy limited by the sideline (cross-talk) effect [Eq. (28)] is independent of $\alpha_0 L$ and therefore should remain unchanged for different gas types (different α_0) and different cell lengths L.

6. Experiments and Results

Experiments were conducted with a two-sensor acetylene detection system (Fig. 1, $N = 2$). The light source was a New-Focus Model 6262 tunable laser with a wavelength tunable from 1518 to 1580 nm. During the experiments, the laser wavelength was tuned to be near a gas absorption line at 1530.2 nm and (frequency) modulated at 500 Hz with a modulation amplitude that was variable from 0 to 22 GHz. The external integrated optic intensity modulator was driven by a VCO that generates a triangular frequency-swept carrier from approximately 65 to 70 MHz with a 10-kHz sweeping rate. The modulation index was estimated to be $\sim m = 0.2$. The two gas cells were of the same length, 2.5 cm. The length of the fiber delay line was ~40 m. The optical path differences between the sensing channels and the electric delay of the reference were adjusted to ensure that the beat frequencies coincided with integer multiples of the sweeping rate. The beat signals generated from the mixer were observed with an electrical spectrum analyzer. Figures 5(a) and 5(b) show, respectively, the spectrum analyzer of the two-sensor system for small (100-MHz) and large (22-GHz) amplitudes of wavelength modulation. The two major peaks, at 10 kHz ($k = 1$) and 30 kHz ($k = 3$), correspond to sensors 1 and sensor 2, respectively. At low modulation amplitudes, $\cos\Delta\psi_{12}$ is in the low-frequency region and appears as sidelines about 10 and 30 kHz. If one now used a bandpass filter to select a particular beat signal, part of the sideband signals that were due to $\cos\Delta\psi_{12}$ would also pass through the filter; i.e., the value of $(\cos\Delta\psi_{12})_B$ in Eq. (4) would be large and therefore affect the measurement accuracy. For large amplitude modulation, $\cos\Delta\psi_{12}$ is in a higher-frequency region and is actu-

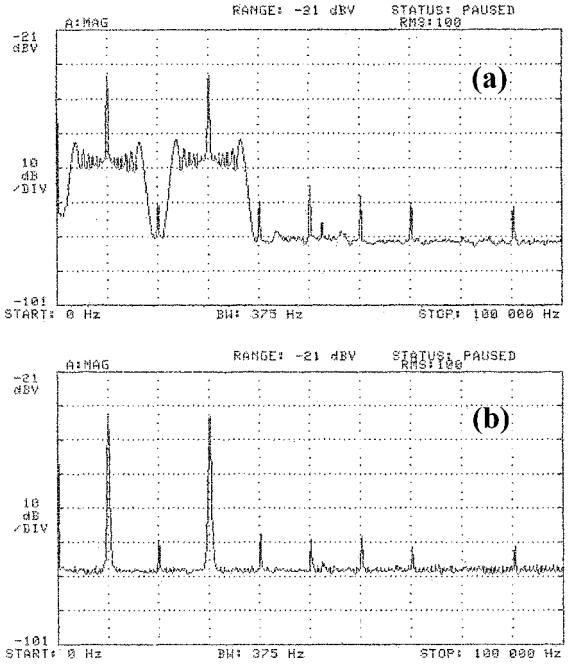

Fig. 5. Output signal spectrum of a two-sensor system. ω_m = 500 Hz. (a) Small modulation amplitude $\nu_{Lm} \approx 100$ MHz, (b) large modulation amplitude $\nu_{Lm} \approx 22$ GHz.

ally out of the range of the spectrum analyzer. The value of $(\cos \Delta\psi_{12})_B$ in Eq. (4) would be much smaller than that for the case of small modulation amplitude. The signal-to-noise ratios near 10 and 30 kHz were improved significantly (20-dB better than with low-amplitude modulation) to 38 dB. The use of large modulation amplitude shifts the coherent mixing signals out of the frequency band of interest and thus reduces the measurement error that is due to $(\cos \Delta\psi_{12})_B$.

Under large amplitude modulation (~20 GHz), the signal at 10 kHz (corresponding to sensor 1) was bandpass filtered and detected by use of a lock-in amplifier with a reference from the 500-Hz wavelength modulation. Figure 6 shows the second-harmonic output

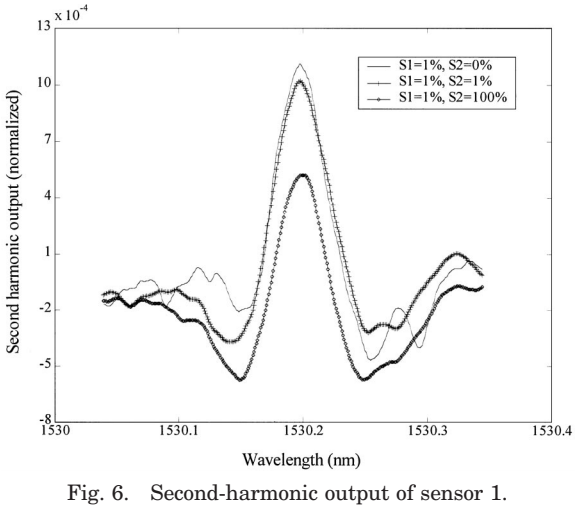

Fig. 6. Second-harmonic output of sensor 1.

when the laser was tuned from 1530.05 to 1530.35 nm with the first sensor cell filled with ~1% acetylene gas. The three curves are the results obtained from three independent wavelength scans when the second sensor cell was filled with 0%, 1%, and 100% acetylene gas. We estimated the minimum detectable gas concentration by comparing the rms value of the noise with that of the signal that was due to 1% acetylene; the concentration was found to be ~165 ppm for 1-s lock-in integration time, corresponding to a minimum detectable absorbance of 2.1×10^{-4}. This value is significantly larger than the theoretical detection sensitivity calculated from expression (26) (or from curve a of Fig. 4) for $N = 2$ (~23 ppm) limited by the unwanted interferometric signals. No variation in detection sensitivity was observed when the light signal from one of the channels was blocked, indicating that the system is not limited by the coherent mixing of signals from different channels. The sensitivity is of the same order as the etalon effect in a single sensor,[21] suggesting that the sensitivity is limited by the etalon effect from the gas cells. We estimated the cross talk by measuring the signal variation in the output of sensor 1 when the second sensor was filled with 0% and 100% acetylene; the cross talk was found to be ~−25 dB. This level of cross talk would result in an error in the detection of gas concentration of $\sim 10^{-2.5} \times 5\% = 0.016\%$ (160 ppm) if a maximum gas concentration of $C_{\max} = 5\%$ were assumed. This value compares well with the simulation result for $N = 2$ and a 0.5-cm bias (curve c of Fig. 4).

7. Summary

We have investigated the performance of a multipoint fiber gas sensor array based on a frequency-modulated continuous-wave (FMCW) technique and wavelength modulation of a tunable external-cavity semiconductor laser. We investigated the limitation imposed on the sensitivity of the fiber gas sensor array by unwanted interferometric signals and by the cross-talk effect that is due to the nonzero sidelines of the FMCW. We showed both experimentally and theoretically how the interferometric effects may be reduced by use of a combination of wavelength modulation–scanning and proper electronic filtering. A two-sensor system with a sensitivity of 165 ppm (or 2.1×10^{-4} in terms of minimum detectable absorbance) and a cross talk of −25 dB was experimentally demonstrated. It is theoretically possible to achieve a 37-sensor array with a detection accuracy of better than 2000 ppm.

Appendix A

1. Derivation of Expression (3)

Assume that the light intensity from the laser at point A as indicated in Fig. 1 is I_A. The electric field at point B in Fig. 1 may be expressed as

$$E_B(t) = \{I_A[1 + m \cos \varphi(t)]\}^{1/2} \exp\left[j2\pi \int_0^t \nu(t)\mathrm{d}t\right], \quad \text{(A1)}$$

where m is the intensity modulation index and $\varphi(t)$ is the phase angle of the intensity modulation applied through the external intensity modulator. $\varphi(t)$ may be related to the instantaneous angular frequency $\omega(t)$ of the VCO by

$$\varphi(t) = \int \omega(t)\mathrm{d}t. \tag{A2}$$

For a triangular chirped carrier with angular frequency excursion $\Delta\omega$ and modulation period T_s, $\omega(t)$ may be written as

$$\omega(t) = \omega_0 + \frac{\Delta\omega}{2} - \left|\frac{2\Delta\omega}{T_s}\left(t - nT_s - \frac{T_s}{2}\right)\right|, \quad t \in [nT_s, (n+1)T], \tag{A3}$$

where ω_0 is the average carrier frequency. After it passes the N-sensor network, the electric field at point C in Fig. 1 may be written as

$$E_c = \sum_{i=1}^{N} E_{ci}, \tag{A4}$$

where E_{ci} ($i = 1, 2, \ldots, N$) represents the electric field at point C after the field passes the ith sensor channel and may be expressed as

$$E_{ci}(t) = (k'I_A)^{1/2}[1 + m\cos\varphi(t_i)]^{1/2} \times \exp\{-\alpha[\nu(t_i)]C_iL\}\exp\left\{j2\pi\int_0^{t_i}\nu(t_i)\mathrm{d}t + \phi[\nu(t_i)]\right\} \tag{A5}$$

and k is a loss factor that depends on the coupling ratio of the couplers used in the network. For simplicity, we have assumed that that loss factor is the same for all the channels and is equal to k. $\phi[\nu(t_i)]$ is the phase modulation that results from gas absorption. It may be neglected for small gas concentration, a short-length gas cell, or both.[9]

The total light intensity at point C may be written as

$$I_c = \langle E_cE_c^*\rangle = \sum_{i=1}^{N}|E_{ci}|^2 + 2\sum_{j=1,j>i}^{N}\mathrm{Re}\langle E_iE_j^*\rangle, \tag{A6}$$

where the first term on the right-hand side is the summation of the light intensities from all the sensors. The second term is the summation of the coherent mixing terms between signals from different channels. Assume first that the signals from different channels are incoherent. The second term would then vanish. The output light intensity $I_c(t)$ at point C may be obtained by substitution of Eq. (A5) into the first term in Eq. (A6):

$$I_c = \sum_{i=1}^{N}|E_{ci}|^2 = k'I_A\sum_{i=1}^{N}\exp[-2\alpha(\nu)C_iL] \times [1 + m\cos\varphi(t_i)]. \tag{A7}$$

The electric signal V_s from the photodetector will then be $V_s = KI_c$, with K representing a conversion coefficient of the photodetector.

The reference signal directly from the VCO may be written as

$$V_r = V_0\cos[\varphi(t_r)], \tag{A8}$$

where $\varphi(t_r)$ is the phase angle of the reference signal. The mixing of V_s and V_r at the mixer produces three different signals that are associated, respectively, with $\cos\varphi(t_r)$, $\cos[\varphi(t_i) + \varphi(t_r)]$, and $\cos[\varphi(t_i) - \varphi(t_r)]$. The first two signals are in a high-frequency region and can be removed by use of a low-pass filter. We are interested here in the phase-difference terms that may be written as

$$V(t) = \tfrac{1}{2}Kk'mGV_0\sum_{i=1}^{N}I_A(t_i)\exp[-2\alpha(\nu)C_iL] \times \cos[\varphi(t_i) - \varphi(t_r)], \tag{A9}$$

where G is the conversion factor of the mixer. There are N terms in Eq. (A9), each corresponding to a different sensing channel. One can obtain $V_F(\omega)$, the spectrum of $V(t)$, by taking the Fourier transform of $V(t)$ and writing it as

$$V_F(\omega) = \sum_{i=1}^{N}V_i'(\omega), \tag{A10}$$

where $V_i(\omega)$ represents the signal spectrum of the ith sensor channel. For a triangular frequency sweep of angular frequency excursion Δf and period T_s, and with small delay difference τ_i, i.e., $\tau_i/T_s \ll 1$, $V_i(\omega)$ can be expressed as[17,18]

$$V_i'(\omega) \approx \tfrac{1}{2}k'KGmV_0I_A\exp[-2\alpha(\nu)C_iL]\sum_{k=0}^{+\infty}\delta(\omega - k\omega_s)4 \times \frac{\sin\{[\omega - (2\Delta\omega/T_s)\tau_i]\,\tfrac{1}{2}(\tfrac{1}{2}T_s - \tau_i)\}}{\omega - (2\Delta\omega/T_s)\tau_i} \times \cos(\omega_0\tau_i - \tfrac{1}{4}\omega T_s)\exp(j\,\tfrac{1}{2}\omega\tau_i), \tag{A11}$$

where $t_i - t_r = \tau_i$ represents a delay-time difference between the signals from the ith sensor and the reference. When Eqs. (1) and (2) are satisfied, the amplitude of the spectrum $V_i(\omega)$ is approximately a single line at $k\omega is$ and can be written as

$$V_i(k\omega_s) = k'KGmV_0I_A\exp[-2\alpha(\nu)C_iL]\left(\frac{T_s}{2} - \tau_i\right) \approx \tfrac{1}{2}k'KGmV_0T_sI_A\exp[-2\alpha(\nu)C_iL], \tag{A12}$$

where we have used the approximation $T_s/2 - \tau_i \approx T_s/2$ because we have assumed that the value of τ_i is small ($\tau_i/T_s \ll 1$). Expression (A12) is expression (3) with $\chi = k'KmGV_0T_s/2$.

2. Derivation of Eq. (4)

The interferometric term is the second term in Eq. (A6) and may be rewritten as

$$I_{c,n}(t) = 2\sum_{i=1,j>i}^{N} \mathrm{Re}\langle E_{ci}E_{cj}^{*}\rangle = 2\sum_{i=1,j>i}^{N} (I_iI_j)^{1/2}[1 + m\cos\varphi(t_i)]^{1/2} \times [1 + m\cos\varphi(t_j)]^{1/2}\cos(\Delta\psi_{ij}), \quad \text{(A13)}$$

with $I_l (l = 1, 2, \ldots, N)$ and $\Delta\psi_{ij}$ given by

$$I_l = [k'I_A]^{1/2}\exp\{-\alpha[\nu(t_l)C_lL]\}, \quad \text{(A14)}$$

$$\Delta\psi_{ij} = 2\pi\int_{t_j}^{t_i}\nu(t)\mathrm{d}t + \Delta\phi_{ij}, \quad \text{(A15)}$$

where $\Delta\phi_{ij}$ is randomly varying owing to environmental disturbances. $I_{c,n}(t)$ depends on the signals from all the channels and varies randomly with environment. The mixing of $V_{c,n}(t) = KI_{c,n}(t)$ with $V_r(t)$ would produce additional signals at the beat frequency of the sensor and therefore introduce errors in the measurement of gas concentration. For small modulation index $m \ll 1$, $I_{c,n}(t)$ can be approximated by

$$I_{c,n}(t) = 2\sum_{i=1,j>i}^{N} (I_iI_j)^{1/2}\{1 + \tfrac{1}{2}m[\cos\varphi(t_i) + \cos\varphi(t_j)]\}\cos(\Delta\psi_{ij}), \quad \text{(A16)}$$

where we have used the approximation

$$[1 + m\cos\varphi(t)]^{1/2} \approx 1 + \tfrac{1}{2}m\cos\varphi(t) \quad \text{(A17)}$$

and have neglected the higher-order term $m^2\cos\varphi(t_i)\cos\varphi(t_j)/4$. The mixing of $V_{c,n}(t) = KI_{c,n}(t)$ with $V_r(t)$ will produce both sum- and difference-frequency terms. The difference-frequency terms of interest here may be written as

$$V_n(t) = \tfrac{1}{2}KmGV_0\sum_{i=1,j>i}^{N}(I_iI_j)^{1/2}\cos(\Delta\psi_{lm}) \times \left\{\sum_{l=i,j}\cos[\varphi(t_l) - \varphi(t_r)]\right\}. \quad \text{(A18)}$$

By following the same process as that from Eqs. (A9)–(A12), we can derive the additional signal at $\omega_i = k\omega_s$, which is due to the unwanted interferometric signals, as

$$V_{i,n}(\omega_i = k\omega_s) = \tfrac{1}{2}KmGV_0\,T_sI_A\sum_{j=1,j\neq i}^{N}\exp[-\alpha(\nu) \times (C_i + C_j)L](\cos\Delta\psi_{i,j})_B. \quad \text{(A19)}$$

Equation (A19) is the same as Eq. (4) with $\chi = k'KmGV_0T_s/2$.

3. Derivation of Eq. (12)

When the wavelength modulation as given in Eq. (5) is applied, the phase term $\Delta\psi_{ij}$ as given in Eq. (A15) can be rewritten as

$$\Delta\psi_{ij} = 2\pi\int_{t_j}^{t_i}\nu_{L0}(t)\mathrm{d}t + 2\pi\nu_{Lm}\int_{t_j}^{t_i}\sin\omega_m t\mathrm{d}t + \Delta\phi = \xi_{ij} + \zeta_{ij}\sin\omega_m(t - \tau_{ji}/2), \quad \text{(A20)}$$

with ξ_{ij} and ζ_{ij} defined in Eqs. (16) and (17), respectively. Substituting Eqs. (A20), (5), and (6) into Eq. (A19), we obtain

$$V_{i,n}(k\omega_s) = \tfrac{1}{2}k'KGmV_0T_sI_0\sum_{j=1,j\neq i}^{N}[(1 + \eta\sin\omega_m t_i)(1 + \eta\sin\omega_m t_j)]^{1/2}\exp\left(-\sum_{l=i,j}\alpha[\nu(t_l)]C_lL \times \{\cos[\xi_{ij} + \zeta_{ij}\sin\omega_m(t - \tau_{ji}/2)]\}_B\right). \quad \text{(A21)}$$

The second harmonic of $V_{i,n}(k\omega_s)$ can be obtained by expansion of Eq. (A21) into a Fourier series. Under the condition that $\alpha(\nu)C_iL \ll 1$, $\eta \ll 1$, and $\omega_m\tau_{ji} \ll 1$, the magnitude of the second harmonic, when the average laser wavelength is at the center of the gas line, is given by Eq. (12).

4. Derivation of Eq. (28)

The second-harmonic signal of sensor i (at $\omega_i = k\omega_s$) is given by expression (9). The second harmonic of the sideline signal at ω_i from the jth channel may be obtained from expressions (A11) and (9) and written as

$$V_{2\omega_m}(\omega_i = k\omega_s)_j = -2k_0k'KGmV_0I_0 \times \frac{\sin[(\Delta\omega/T_s)(\tau_i - \tau_j)(\tfrac{1}{2}T_s - \tau_j)]}{(\Delta\omega/T_s)(\tau_i - \tau_j)} \times \cos(\omega_0\tau_j - \tfrac{1}{2}\Delta\omega\tau_i)\alpha_0C_jL. \quad \text{(A22)}$$

The total second harmonic at $\omega_i = k\omega_s$ for an N-sensor system can be expressed as

$$V_{2\omega_m}{}^{N}(\omega_i)_j = \sum_{j=1,j\neq i}^{N}V_{2\omega_m}(\omega_i)_j = 2k_0k'KGmV_0I_0\alpha_0L\sum_{j=1,j\neq i}^{N}M_jC_j, \quad \text{(A23)}$$

where M_j is defined in Eq. (29). By setting the signal given by Eq. (A23) equal to that given by expression (9), we obtain Eq. (28).

This study is supported by the Hong Kong Special Administrative Region (SAR) government through Competitive Earmarked Research Grant (CERG)

grant PolyU 5081/98E(B-Q242) and the Hong Kong Polytechnic University through grant (G-V591).

References

1. G. Stewart, "Fibre optic sensors," in *Sensor Technologies*, Vol. 1 of Sensor Systems for Environmental Monitoring, M. Campbell, ed. (Chapman & Hall, London, 1997), Chap. 1, pp. 1–40.
2. J. P. Dakin, C. A. Wade, D. Pinchbeck, and J. S. Wykes, "A novel optical fibre methane sensor," J. Opt. Sensors **2,** 261–267 (1987).
3. K. Chan, H. Ito, H. Inaba, and T. Furuya, "10 km-long fiber optic remote sensing of CH_4 gas by near infrared absorption," Appl. Phys. B **38,** 11–15 (1985).
4. D. M. Bruce and D. T. Cassidy, "Detection of oxygen using short external cavity GaAs semiconductor diode lasers," Appl. Opt. **29,** 1327–1332 (1990).
5. D. B. Oh and D. C. Hovde, "Wavelength-modulation detection of acetylene with near-infrared external-cavity diode laser," Appl. Opt. **34,** 7002–7005 (1995).
6. X. Zhu and D. T. Cassidy, "Electronic subtracter for trace-gas detection with InGaAsP diode laser," Appl. Opt. **34,** 8303–8308 (1995).
7. J. A. Silver, "Frequency-modulation spectroscopy for trace species detection: theory and comparison among experimental methods," Appl. Opt. **31,** 707–717 (1992).
8. D. S. Bomse, A. C. Stanton, and J. A. Silver, "Frequency-modulation and wavelength modulation spectroscopies: comparison of experimental methods using a lead-salt diode laser," Appl. Opt. **31,** 718–731 (1992).
9. W. Jin, Y. Z. Xu, M. S. Demokan, and G. Stewart, "Investigation of interferometric noise in fiber-optic gas sensors with use of wavelength modulation spectroscopy," Appl. Opt. **36,** 7239–7246 (1997).
10. J. Reid and D. Labrie, "Second-harmonic detection with tunable diode lasers—comparison of experiment and theory," Appl. Phys. B **26,** 203–210 (1981).
11. B. F. Ventrudo and D. T. Cassidy, "Operating characteristics of a tunable diode laser absorption spectrometer using short-external-cavity and DFB laser diodes," Appl. Opt. **29,** 5007–5013 (1990).
12. Y. Shimose, T. Okamoto, A. Maruyama, M. Aizawa, and H. Nagai, "Remote sensing of methane gas by differential absorption measurement using a wavelength-tunable DFB LD," IEEE Photon. Technol. Lett. **3,** 86–87 (1991).
13. G. Stewart, C. Tandy, D. Moodie, M. A. Morante, and F. Dong, "Design of a fiber optic multipoint sensor for gas detection," Sensors Actuators B **51,** 227–232 (1998).
14. W. Jin, "Performance analysis of a time-division-multiplexed fiber-optic gas-sensor array by wavelength modulation of a distributed-feedback laser," Appl. Opt. **38,** 5290–5297 (1999).
15. J. P. Dakin, "Multiplexed and distributed optical fiber sensors," J. Phys. E **20,** 954–967 (1987).
16. J. L. Brooks, B. Moslehi, B. Y. Kim, and H. J. Shaw, "Time-domain addressing of remote fiber-optic interferometric sensor arrays," J. Lightwave Technol. **LT-5,** 1014–1023 (1987).
17. P. K. C. Chan, W. Jin, J. M. Gong, and M. S. Demokan, "Multiplexing of fiber Bragg grating sensors using an FMCW technique," IEEE Photon. Technol. Lett. **11,** 1470–1472 (1999).
18. P. K. C. Chan, "Multiplexing of fiber optic bragg grating sensors," Ph.D. dissertation (Hong Kong Polytechnic University, Hong Kong, 2000).
19. H. Riris, C. B. Carlisle, R. E. Warren, and D. E. Cooper, "Signal-to-noise ratio enhancement in frequency-modulation spectrometers by digital signal processing," Opt. Lett. **19,** 144–146 (1994).
20. C. C. Chan, "Interrogation of fiber Bragg grating sensors with a tunable laser," Ph.D. dissertation (Hong Kong Polytechnic University, Hong Kong, 2000).
21. W. R. Philp, W. Jin, A. Mencaglia, G. Stewart, and B. Culshaw, "Interferometric noise in frequency modulated optical gas sensors," in *Proceedings of Twenty-First Australian Conference on Optical Fibre Technology* (Institute of Radio and Electronics Engineers Society, Milsons Point, Australia, 1986), pp. 185–188.